BESS-Polar II Measurements of the Cosmic-ray Proton and Helium Spectra at Solar Minimum

K. SAKAI[1,*], K. ABE[2,†], H. FUKE[3], S. HAINO[4,‡], T. HAMS[1,*], M. HASEGAWA[4], A. HORIKOSHI[4], K. C. KIM[5], A. KUSUMOTO[2], M. H. LEE[5], Y. MAKIDA[4], S. MATSUDA[4], Y. MATSUKAWA[2], J. W. MITCHELL[1], J. NISHIMURA[6], M. NOZAKI[4], R. ORITO[2,§], J. F. ORMES[7], M. SASAKI[1,*], E. S. SEO[5], R. SHINODA[6], R. E. STREITMATTER[1], J. SUZUKI[4], K. TANAKA[4], N. THAKUR[1], T. YAMAGAMI[3], A. YAMAMOTO[4], T. YOSHIDA[3], K. YOSHIMURA[4,¶]

[1] *NASA-Goddard Space Flight Center (NASA-GSFC), Greenbelt,MD 20771, USA*
[2] *Kobe University, Kobe, Hyogo 657-8501, Japan*
[3] *Institute of Space and Astronautical Science, Japan Aerospace Exploration Agency (ISAS/JAXA), Sagamihara, Kanagawa 229-8510, Japan*
[4] *High Energy Accelerator Research Organization (KEK), Tsukuba, Ibaraki 305-0801, Japan*
[5] *IPST, University of Maryland, College Park, MD 20742, USA*
[6] *The University of Tokyo, Bunkyo, Tokyo 113-0033, Japan*
[7] *University of Denver, Denver, CO 80208, USA*
[*] *also at: Center for Research and Exploration in Space Science and Technology (CRESST)*
[†] *now at: ICRR, Tokyo*
[‡] *now at: National Central University*
[§] *now at: Tokushima University*
[¶] *now at: Okayama University*

kenichi.sakai@nasa.gov

Abstract: The energy spectra of cosmic-ray protons and helium near solar minimum were precisely measured with BESS-Polar II (Balloon-borne Experiment with a Superconducting Spectrometer) during a long-duration flight over Antarctica in December 2007 and January 2008, and are discussed here. The absolute fluxes and spectral shapes of primary protons and helium probe the origin and the propagation history of cosmic rays in the Galaxy. The spectra are also essential as inputs to calculate the spectrum of cosmic-ray antiprotons, which are secondary products of cosmic-ray interactions with the interstellar gas. To optimize the measurement of the magnetic rigidity of incident particles, obtained from the curvature of their trajectories in a solenoidal magnetic field of 0.8 Tesla, an improved calibration of the central JET-type drift chamber and two inner drift chambers was developed. Using this, we obtained absolute spectra of primary cosmic-ray protons up to around 120 GeV and helium up to around 50 GeV/nucleon.

Keywords: Cosmic-ray proton, Cosmic-ray helium, Superconducting spectrometer, Solar minimum

1 Introduction

The absolute flux and spectral shape of primary cosmic rays are the basis for understanding the origin and the propagation history of the cosmic rays in the Galaxy. The proton and helium spectra are also essential as inputs to calculations of the spectra of cosmic-ray antiprotons and positrons which are secondary products of cosmic-ray interactions with the interstellar gas. During propagation through the ISM cosmic rays undergo interactions with gas atoms and loose energy, significantly modifying their spectra and composition. Then when Galactic cosmic rays enter the heliosphere, they are scattered by irregularities in the heliospheric magnetic field and undergo convection and adiabatic deceleration in the expanding Solar wind. This process, modifying the energy spectra of cosmic rays, is known as “Solar modulation”.

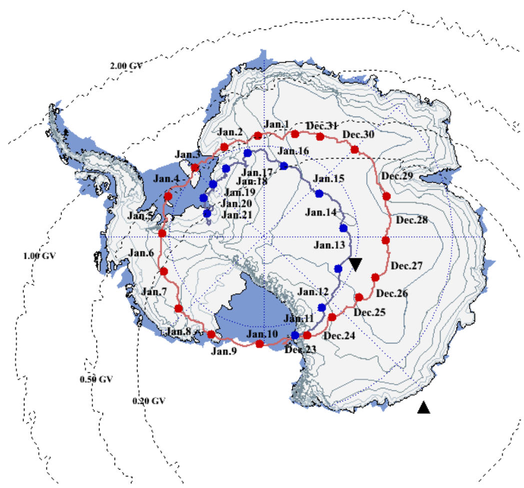

Figure 1: Flight trajectory of the 2007 BESS-Polar II over Antarctica from Williams Field.
[Launch]S77-51,E166-40, 06:27(McM) 12/23 2007
[Recovery]S83-51,W073-04, 09:02(UTC) 1/21 2008

2 BESS Program

The BESS instrument [1, 2] was developed as a high-resolution magnetic-rigidity spectrometer for cosmic-ray antiparticles and precise measurements of the absolute fluxes of various cosmic-ray components. The original BESS experiment performed 9 flights over northern

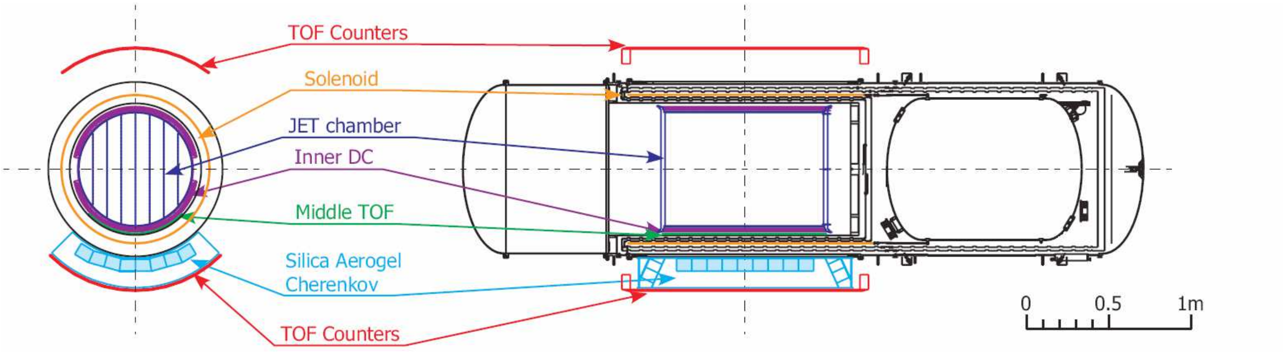

Figure 2: Cross sectional view of BESS-Polar II spectrometer

Canada during the period of 1993 through 2002 with continuous improvement in the instrument [3]. The BESS-Polar project was proposed as an advanced BESS program using long duration balloon (LDB) flights over Antarctica (around the south pole) to provide high-statistics, low-energy cosmic-ray measurements [4, 5, 6]. The first scientific flight of the BESS-Polar instrument was launched near McMurdo Station, on December 13th, 2004 (UTC). The flight duration was over 8.5 days and more than 9×10^8 cosmic-ray events were recorded [7].

Incorporating considerable improvements in instrument and payload systems compared to BESS-Polar I, the BESS-Polar II instrument was launched on December 23, 2007, from Williams Field near the US McMurdo Station in Antarctica and circulated around the South Pole for 24.5 days of observation with the magnet energized. The float altitude was 34 km to 38 km (residual air of 5.8 g/cm^2 on average), and the cutoff rigidity was below 0.5 GV. BESS-Polar II accumulated 4.7×10^9 events with no inflight event selection as 13.6 terabytes of data (Fig.1).

The BESS-Polar II program has produced two papers giving precise measurements of antiprotons [8] and a sensitive antihelium search [9]. The antiproton spectrum measured by BESS-Polar II shows good consistency with secondary antiproton calculations and no evidence of primary antiprotons originating from the evaporation of primordial black holes. And antihelium work has set a new limit in the ratio of possible antihelium to measured helium of 6.9×10^{-8} at 95% confidence, the lowest limit to date.

3 BESS-Polar Instrument

In the BESS-Polar instruments, a uniform field of 0.8 T is produced by a thin superconducting solenoid, and the field region is filled with drift-chamber tracking detectors. Tracking is performed by fitting up to 52 hit points with a characteristic resolution of $\sim 140\mu$m in the bending plane, resulting in a magnetic-rigidity ($\equiv Pc/Ze$) resolution of 0.4% at 1 GV and a maximum detectable rigidity (MDR) of 270 GV. Upper and lower scintillator hodoscopes provide time-of-flight (TOF) and dE/dx measurements and the event trigger. For antiproton measurements, the acceptance of BESS-Polar is 0.23 m^{2}sr and for proton and helium measurements the acceptance is 0.18 m^{2}sr. The timing resolution of the TOF system is 120 ps, giving a β^{-1} resolution of 2.5%. The instrument also incorporates a threshold-type Cherenkov counter using a silica aerogel radiator with index $n = 1.03$ (ACC) that can reject e^- and μ^- backgrounds by a factor of 12000 and distinguish $\bar{p}$'s from such backgrounds up to 3.5 GeV. In addition, a thin scintillator middle-TOF (MTOF) is installed on the lower surface of the solenoid bore to detect low-energy particles which cannot penetrate the magnet wall. The timing resolution using the MTOF is 320 ps. The MTOF was employed to verify the procedure used to eliminate contamination from events in which interacting protons mimic low-energy $\bar{p}$'s.

4 Solar Modulation

The considerable variation in solar activity and details of the affect of the solar wind and its entrained magnetic fields on the incoming GCR fluxes have to be taken into account in deriving interstellar spectra. Figure 3 shows evidence of Solar modulation of cosmic rays and Solar activity illustrated by the changes with time of the Bartol neutron monitor counting rate (Blue points) [10] and the number of sunspots (Red points) [11] together the data of BESS flights. The Solar cycle has an approximately 11-year period. In addition, the sun has a 22 year magnetic cycle with recurrent positive ($A > 0$) and negative ($A < 0$) phases, where $A < 0$ polarity cycles are defined as the periods when the heliospheric magnetic field (HMF) is directed towards the Sun in the

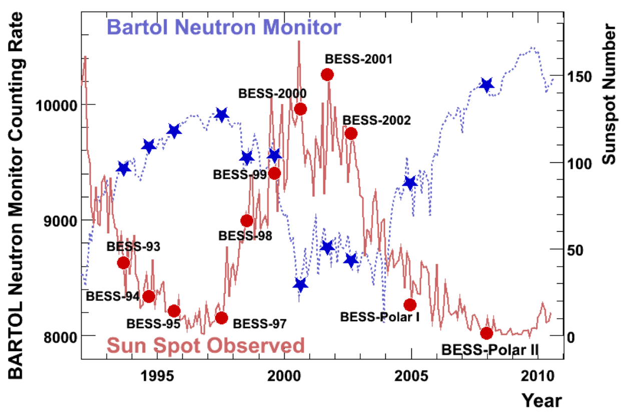

Figure 3: Variation of neutron monitor and sunspot number together the data of BESS flights. The BESS-Polar II flight was carried out near the absolute Solar minimum.

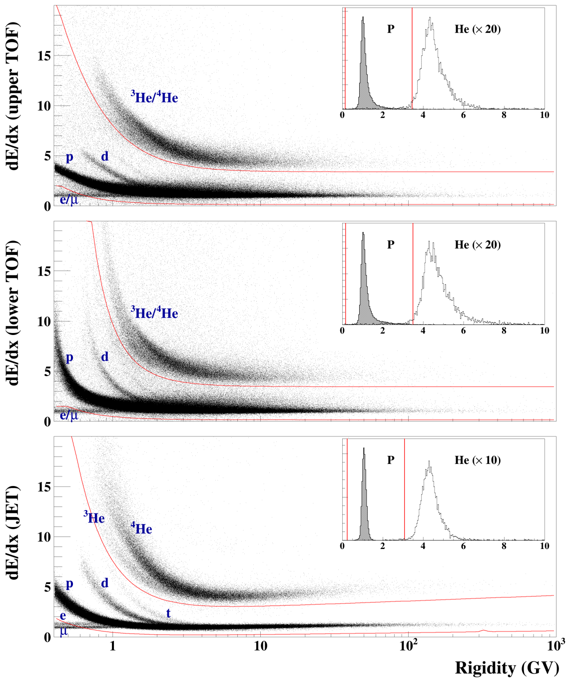

Figure 4: Proton band in dE/dx (top: upper TOF, middle: lower TOF, bottom: JET) vs. rigidity obtained from the balloon observation. The superimposed graph shows the selection criteria for protons and helium nuclei above 10 GV.

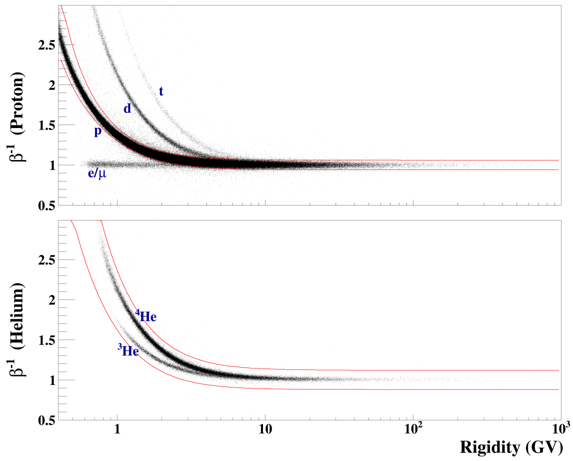

Figure 5: Scatter plot of β^{-1} vs. rigidity obtained from the balloon observation after proton and helium dE/dx selection.

northern hemisphere. The magnetic field polarity reverses when the Solar activity is maximum, and the global magnetic field profile also reverses in the heliosphere. The positive and negative particles traversing the HMF drift in opposite directions, taking different routes to arrive at the Earth. This explains the alternate appearances of ”flat” and ”peaked” periods in neutron monitor data around Solar ”minimum”. Since the low-energy region of the cosmic radiation is most intensively affected by Solar modulation, the absolute fluxes and spectral shapes of primary protons and helium obtained with BESS are essential probes of Solar modulation. These are combined with the simultaneous BESS antiproton measurements to probe the effect of charge-sign dependent drift on the entering cosmic rays.

5 Data analysis

In the first stage of data analysis, we selected events with a single track fully contained inside the fiducial volume defined by the central four columns out of eight columns in the JET chamber. This definition of the fiducial volume reduced the effective geometrical acceptance down to $\sim \frac{1}{3}$ of the full acceptance, but it ensured the longest track fitting and thus the highest resolution in the rigidity measurement. A single-track event was defined as an event which has only one isolated track and one or two hit counters in each layer of the TOF hodoscopes. The single-track selection eliminated rare interacting events. The single-track selection eliminated rare interacting events. To estimate the efficiency of the single-track selection, Monte Carlo simulations with GEANT3/4 were performed.

5.1 Event selection

Particle identification was performed by requiring proper dE/dx measurements with both upper and lower layers of the TOF hodoscopes and β^{-1} as functions of rigidity. Figs. 4 and 5 show the selection criteria for protons and helium. The efficiencies of dE/dx selection were estimated with another sample selected by independent measurement of energy loss inside the JET. Since the β^{-1}distribution is well described by Gaussian and a halfwidth of the β^{-1} selection band was set at 4σ the efficiency is very close to unity.

5.2 Normalization and corrections

$$\Phi_{\mathrm{TOA}}(E_{\mathrm{TOA}}) = \frac{\Phi_{\mathrm{TOI}}(E_{\mathrm{TOI}})}{\eta(E_{\mathrm{TOI}\rightarrow\mathrm{TOA}}) + R_{\mathrm{air}}(E_{\mathrm{TOI}\rightarrow\mathrm{TOA}})} \quad (1)$$

$$\Phi_{\mathrm{TOI}}(E_{\mathrm{TOI}}) = N_{\mathrm{p}}/(\varepsilon_{\mathrm{det}} \cdot \varepsilon_{\mathrm{non-int}})/(S\Omega \cdot T_{\mathrm{live}}) \quad (2)$$

where N_{p} is number of observed proton, $\varepsilon_{\mathrm{det}}$ is detection efficiency that is related to the event selection, $\varepsilon_{\mathrm{non-int}}$ is non interaction efficiency, $S\Omega$ is geometrical acceptance and T_{live} is the live time period. $(1-\eta)$ is losses in the atmosphere and R_{air} is atmospheric secondary production.

In order to determine the primary cosmic-ray proton and helium spectra at the top of the atmosphere, the following normalization and corrections are required : (1) exposure factor, (2) ionization energy loss, (3) interaction loss, and (4) atmospheric secondary particle contribution.

The exposure factor is a product of geometrical acceptance and live time. The geometrical acceptance defined for this analysis was calculated by simulation technique. The simple cylindrical shape and the uniform magnetic field make it simple and reliable to determine the geometrical acceptance precisely. The live data-taking time was measured to be 1.3×10^6 s. The energy of each incoming particle was calculated by integrating the energy losses inside the detector tracing back along the particle trajectory. In order to obtain the absolute flux of primary protons and helium nuclei at the top of the atmosphere, interaction loss and secondary particle production in the residual atmosphere were estimated. Both for air correction can be estimated by solving simultaneous transport equations following Papini et al

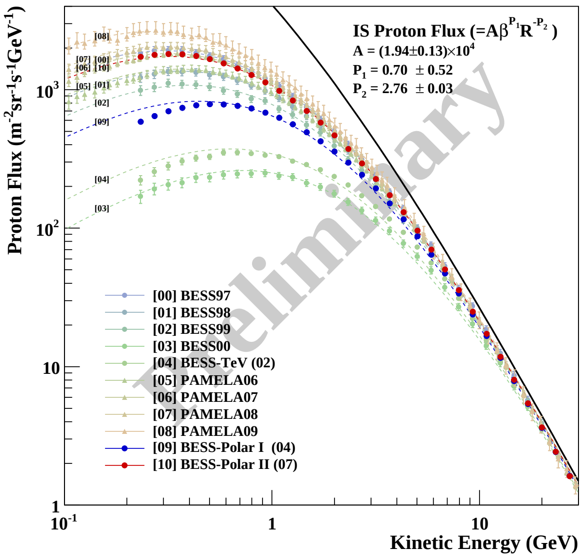

Figure 6: Absolute differential energy spectrum of primary protons obtained from BESS-Polar II. The spectra obtained by other experiments [13, 14, 15, 16, 17] are also shown.

[12]. The primary spectrum at TOA (Φ_{TOA}) is determined in an iterative procedure so that the estimated spectrum at TOI (Φ_{TOI}) agrees with the observed one.

6 Measured Spectra

In the present work, we have obtained the absolute fluxes of primary protons in the range 0.2-120 GeV and helium nuclei in the range 0.2-50 GeV/n at the top of the atmosphere from the BESS-Polar II balloon-flight data in 2007. The overall uncertainties including both statistical and systematic errors were less than $\pm 15\%$ for protons, $\pm 20\%$ for helium nuclei. The results of primary proton spectrum are shown in Fig. 6 in comparison with other experiments with magnetic spectrometers.

In Fig. 6, a Force Field approximation is employed to compare measured spectra with those calculated using the BESS interstellar spectrum (IS). In this model, cosmic-ray spectra at various solar activities are described by the IS proton spectrum and one "modulation parameter". The solar wind is assumed to be spherically symmetric and is described with a simplified diffusion co-efficient and a transport equation for the propagation of cosmic-ray charged particles. The IS proton spectrum was assumed to be described with $A\beta^{P_1}R^{-P_2}$, where, as usual, β is the velocity of the particle divided by speed of light, R is the rigidity, and A , P_1 and P_2 are the fitting parameters. The parameter ϕ for BESS-1998 was estimated to be $\sim$ 600 MV by Myers et al. Other curves and values of ϕ were obtained by fitting the measured spectra shown using the common IS proton spectrum (Shown in Fig.6).

The Force Field approximation fits relatively well to the spectra measured in 1997, 1998 and 1999, which are in the positive phase of the Sun's magnetic field polarity. However, obvious discrepancies can be seen in 2002 (BESS-TeV) and 2004 (BESS-Polar I), which are in the negative phase and far from solar minimum. The drift pattern of charged particles coming into the heliosphere varies with the sign of the polarity of heliospheric magnetic field. This feature cannot be treated in the Force Field approximation. Furthermore, the amount of energy loss depends on the observed particle energy, especially for negative polarity phase. The small discrepancy seen in 2002 and 2004 may come from an inadequacy of the assumption of the model that the energy loss is independent of energy.

7 Conclusion

At the time of writing we have measured energy spectra of primary protons in the range 0.2-120 GeV by BESS-Polar II. This work will be extended to include the energy spectra of helium nuclei. The $\bar{p}/p$ ratio obtained by BESS-Polar II using the measured proton spectrum will be given in a separate paper [3].

The low energy cosmic-ray proton and helium spectra and the solar modulation effects have been much better understood based on the measurements with the BESS spectrometer.

Acknowledgements

The BESS-Polar program is a Japan-United States collaboration, supported in Japan by the Grant-in-Aid 'KAKENHI' for Specially Promoted and Basic Researches, MEXT-JSPS, and in the U.S. by NASA. Balloon flight operations were carried out by the NASA Columbia Scientific Balloon Facility and the National Science Foundation United States Antarctic Program. We would like to express our sincere thanks for their continuous professional support.

References

[1] Y. Ajima et al., Nucl. Instrum. Meth., **A443** 71 (2000).
[2] S. Haino et al., Nucl. Instrum. Meth., **A518** 167 (2004).
[3] J. W. Mitchell et al., ICRC 2013: Rio de Janeiro, ID: 1087 (2013).
[4] A. Yamamoto, Adv. Space Res., **30** 1253 (2002).
[5] J. W. Mitchell et al., Nucl. Phys. (Proc. Suppl.), **134** 31 (2004).
[6] T. Yoshida, Adv. Space Res., **33** 1755 (2004).
[7] K. Abe et al., Phys. Lett., **B670** 103 (2008).
[8] K. Abe, Phys. Rev. Lett., **108** 051102 (2012).
[9] K. Abe, Phys. Rev. Lett., **108** 131301 (2012).
[10] ftp://ftp.bartol.udel.edu/pyle/BRIData/.
[11] http://solarscience.msfc.nasa.gov/greenwch/.
[12] P. Papini, C. Grimani, S. A. Stephens, Nuovo Cim., **C19** 367 (1996).
[13] T. Sanuki, The Astrophysical Journal, **545** 1135 (2000).
[14] K. Abe, Physics Letters B, **564** 8 – 20 (2003).
[15] S. Haino et al., Phys. Lett., **B594** 35 (2004).
[16] Y. Shikaze et al., Astropart. Phys., **28** 154 (2007).
[17] O. Adriani, The Astrophysical Journal, **765** 91 (2013).